J|A|C|S COMMUNICATIONS

Published on Web 09/29/2009

Surface-Enhanced Raman Scattering Captures Conformational Changes of Single Photoactive Yellow Protein Molecules under Photoexcitation

Kushagra Singhal and A. Kaan Kalkan*

School of Mechanical and Aerospace Engineering, Oklahoma State University, Stillwater Oklahoma 74078

Received April 9, 2009; E-mail: kaan.kalkan@okstate.edu

Proteins are the machinery of life. They perform all the fundamental functions in biosystems, from reception of antigens in the immune system to sensing of light in vision. Proteins carry out their jobs through a series of transient conformational states. These structural movements involve a diversity of pathways and distribution of time scales from one protein molecule to another. Such "molecular individuality" is, however, averaged out and masked by ensemble-averaged measurements.[1]

In 1997, demonstration of Surface-Enhanced Raman Scattering (SERS) from single molecules hinted at the opportunity of resolving protein structure−activity relationships at the Single Molecule (SM) level.[2,3] Since then, however, only one study exploited SERS to "watch" single protein molecules "in action". Namely, Habuchi et al. monitored dynamic conversion of green fluorescent protein between protonated and deprotonated forms.[4] SM-SERS detection of two other proteins, hemoglobin and horseradish peroxidase, was also achieved, though without monitoring the conformational dynamics.[5,6]

In this Communication, we report capturing the distinct conformational changes of a photoreceptor protein, photoactive yellow protein (PYP) under photoexcitation, at the single molecule level, using SERS substrates. PYP is a small (14 kDA) cytosolic photoreceptor protein, extracted from *Halorhodospira halophila*, with 125 amino acid residues.[7,8] As illustrated in Figure 1a, in its ground state (pG), PYP has a para-Coumaric Acid (pCA) chromophore, covalently bound to the side chain of cysteine (Cys69) through a thiolester linkage, and its deprotonated phenolic oxygen is stabilized by a H-bond network with protonated Glu46 and Tyr42.[9,10] The photocycle of PYP is initiated by the absorption of a blue photon (absorption peak at 446 nm) by the pCA. The absorbed energy thereafter thermalizes through a chain of conformational states.[11]

Our "nanometal-on-semiconductor" SERS substrates are prepared by reduction of Ag^+ on Ge thin films.[12] Once 1 μL aliquots of PYP (10^{-9} M, pH 7) are spotted and a 514 nm laser probe is focused at the aliquot/substrate interface, single molecule spectra are observed in terms of the sudden appearance of discernible Raman peaks over a weak background.[13,14] On the average, these spectral jumps occur every several seconds and sustain for ~1 s as depicted by Figure 1b. The wavenumber and relative intensity of the intermittent peaks show random deviations from those of the ensemble-averaged spectrum (e.g., 10^{-7} M PYP). In addition, a dramatic decrease in inhomogeneous line width is evidenced for certain peaks. Hence, absence of statistical averaging is inferred in our intermittent spectra, and we associate them with single PYP molecules diffusing in and out of SERS hot spots (typical enhancement factor: 4×10^{10}). In particular, spectral shifts described above are attributed to statistical fluctuations in the chemisorption configuration and local environment of the molecule.[2,6,14,15] Time series spectra are collected with a signal integration time of 0.25 s, being shorter than PYP's photocycle (0.35 s). When employing a Renishaw RM 1000 Raman spectrometer, each 0.25 s scan is followed by a shutter/read-out time of 1 s that only permits us to monitor the structural dynamics of PYP intermittently. Nevertheless, an SM spectrum integrated for 0.25 s serves like the "molecule's logbook" and records the structural steps taken by the molecule in that duration.

Figure 1 displays a series of such "logs" reported by different PYP molecules while they temporarily occupied "high- enhancement sites". These spectra capture different steps that are instrumental in the photocycle. Figure 1c shows the shift of the υC8−C9 (stretching) mode from 1056 to 1010 cm^{-1} which is indicative of the chromophore undergoing photoisomerization to *cis* about the C7═C8 bond.[16−18] Photoisomerization involves breaking of the H-bond between O2 and the amide group of Cys69 as well as a carbonyl (C9═O2) flip[19] accounting for the red-shifted intermediate state: pR. The structural model for pR is given in Figure 1d. pR is marked by the 1665 cm^{-1} peak, which is assigned to the υC9═O2 (stretching) mode. At the ground state (pG), this mode is observed at 1630 cm^{-1}.[16,18] It is seen at 1638 cm^{-1} in the single molecule spectrum of Figure 1e. Accordingly, Figure 1e captures the carbonyl flip, suggestive of pG to pR transition in a single PYP molecule.

It may appear uncertain whether a spectrum as such as that in Figure 1 records a transition in a single molecule or rather if the spectra of two molecules in different states are integrated. When Raman scattered radiation (10^{-9} M PYP) is imaged with a CCD video camera, bright blinking spots are recorded on a faint background. The temporal nature of this blinking matches with that of spectral jumping. Accordingly, the spots are attributed to diffraction limited Raman images of the single molecules. Further, the blinking spots are typically observed to occur several seconds apart. Therefore, it is unlikely that a 0.25 s acquisition can accumulate signals from two molecules.

Conversion to pR triggers a proton transfer from Glu46 to phenolic $O1^-$, as illustrated in Figure 1d.[20] The proton transfer is a crucial step in the photocyle, as the resultant unstable buried charge of $Glu46^-$ is considered to drive the unfolding of the protein in the creation of the blue-shifted signaling state (pB).[21−23] This significant conformational change in the protein structure provides biological signal transduction that lasts for ~0.35 s before PYP recovers to pG and completes the photocycle.[11,24] As captured for single PYP molecules in Figure 1c and 1f, protonation is observed through, at least, three different markers: (i) shift in υC7═C8, υCC mode (containing the vinyl bond stretching and the ring vibrations) from 1534/1555 to 1576/1599 cm^{-1}; (ii) shift in δCH mode (aromatic ring motion) from 1163 to 1174 cm^{-1}; and (iii) shift in υCC, υC7═C8 mode (involving the ring vibrations and the vinyl bond stretching) from 1495 to 1515 cm^{-1}.[16−18]

Figure 2a shows an SM-SERS spectrum complying with pG. Also provided is an Ensemble-Averaged (EA) SERS spectrum. In the absence of statistical averaging, SM-SERS yields well-resolved, sharp peaks.[14,15] In contrast, EA-SERS is not capable of resolving

10.1021/ja9028704

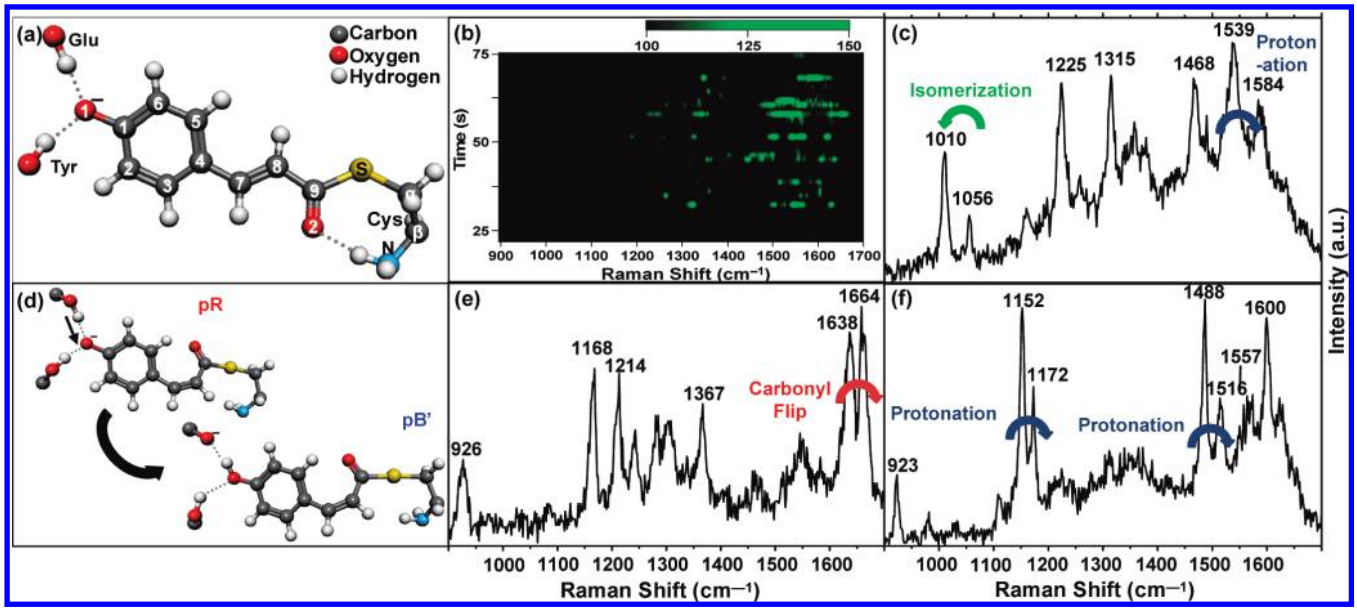

Figure 1. (a) PYP chromophore structure at ground state (pG) with neighboring amino acid residues. (b) Waterfall plot illustrating spectral fluctuations observed in temporal single molecule spectra ("spectral jumps"). (c) SM-SERS spectra capturing photoisomerization to cis and protonation. (d) Structural models illustrating protonation of the chromophore: transition from pR to pB. pB′ represents the onset of pB before signaling (unfolding) starts. SM-SERS spectra capturing: (e) Carbonyl flip with breaking of H-bond; (f) Protonation as observed from two markers.

cis/trans, protonation, and carbonyl flip markers due to heterogeneous broadening. In particular, the SM spectrum in Figure 2a shows a well-resolved peak at 1204 cm^{-1}, which is only seen as a weak shoulder in the EA spectrum. Interestingly, this mode was not observed in earlier Raman or time-resolved Raman studies and only predicted by theoretical calculations (υC4−C7 mode).[16] Another such peak is at 1346 cm^{-1}, estimated to belong to υC1−O1 in pG.[16] Possibly, these Raman-inactive modes become SERS-active by modified selection rules due to chemisorption-induced symmetry lowering and mixing of pCA and Ag states.[25−27]

Figure 2b compares the average of 385 SM-SERS spectra with EA-SERS. We attribute the remarkable spectral diffusion in averaged SM-SERS to pCA-Ag electron transfer (wave function mixing), which also accounts for the chemical enhancement (i.e., 10^2−10^4) needed to detect single molecules.[2,28] Variations in PYP's chemisorption configuration on Ag are expected to lead to variations in pCA-Ag electron transfer and variations in bond force constants resulting in heterogeneous peak broadening.[15,25,27] As mentioned earlier, the electron transfer also allows new modes to be Raman-active making the averaged SM-SERS spectrum more difficult to resolve. Whereas, the EA-SERS signal is averaged dominantly from lower enhancement sites, where electron transfer effects and hence said spectral diffusion are to a lesser degree.[2,15]

Further evidence for chemisorption is deduced from differential optical absorption, when semitransparent Ag films (i.e., 12 nm thick) are immersed in 10^{-6} M PYP. As seen in Figure 3, a dramatically red-shifted and broadened band emerges in comparison with the 446 nm peak found for PYP in water. In view of the "adsorbate-induced states" model, this remarkable change in distribution of states is attributed to mixing of metal and molecular electronic states.[29] The red shift and broadening allow resonant excitation of the pCA chromophore at 514 nm that accounts for not only additional (chemical) enhancement in SERS but also activation of PYP's photocycle (i.e., photoisomerization in pCA) by green (i.e., 514 nm) photons.

Although multiple markers identify a certain conformational state, not all appear in the same SM-SERS spectrum. For example, when the ∼1200 cm^{-1} peak (υC4−C7, pG) is strong, the 1630 cm^{-1} peak (υC9═O2, pG) is weak as seen in Figure 2a, and vice versa. Figure 4 depicts this inverse correlation with a histogram based upon 100 spectra, each of which captured at least one of the two peaks. In the horizontal axis, the "ratio" denotes the lower peak intensity divided by larger peak intensity that lies between 0 and 1. A normally expected peak can be absent or subdued if its associated Raman transition moment is misaligned with the enhanced electric field, which is normal to the metal surface in the hot spot.[26,27,30] Whereas, vibrational modes, which induce transition moments well aligned with the enhanced field, can lead to intense Raman scattering. The alignment is simply determined by the chemisorption configuration of the molecule. Given the signal is from a single molecule, the exclusive trend between the υC4−C7 (pG) and υC9═O2 (pG) peaks, therefore, suggests the transition moments

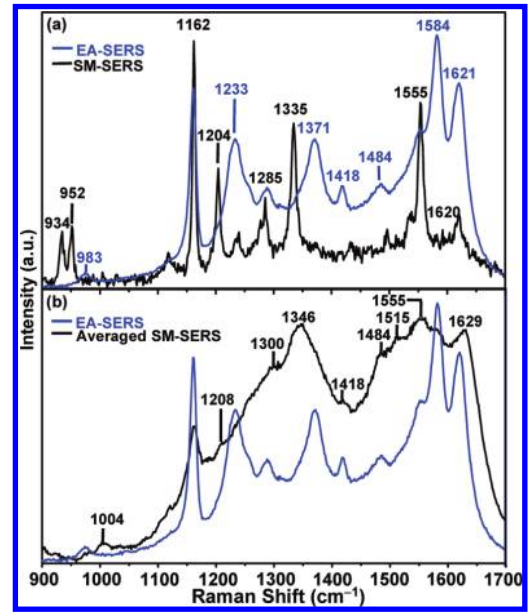

Figure 2. (a) SM-SERS spectrum characteristic of pG and comparison with EA-SERS. (b) Averaged SM-SERS compared with EA-SERS.

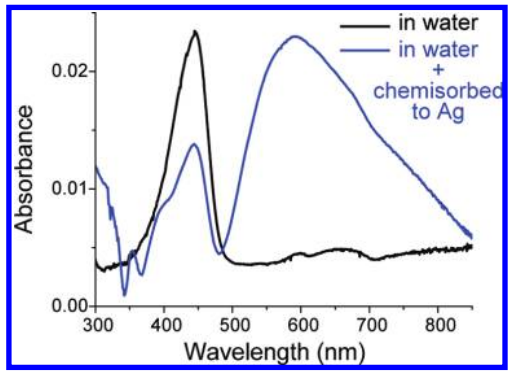

Figure 3. Optical absorption: PYP in water (2.0×10^{-6} M); PYP in water (1.0×10^{-6} M) and chemisorbed to silver.

of the modes are orthogonal. Additionally, PYP must have two typical adsorption configurations on Ag. For each configuration, only one of the transition moments must align with the electric field.

Similarly, υC9═O2 is generally found to be exclusive with υC8─C9, as seen in Figure 1c and 1e. In other words, trans-to-cis and carbonyl flip markers do not usually coexist as in Figure 1c and 1e, although both spectra capture a pG to pR transition. On the other hand, neither υC9═O2 nor υC8─C9 is observed with significant intensity in Figure 1f, which cannot be explained by orthogonal transition moments. The absence of peaks in SM-SERS may also result from selective turning down of the chemical enhancement for that particular mode. Chemical enhancement is attributed to mixing of metal and molecule wave functions. Thus, if the vibrational mode is localized (e.g., around a bond), chemical enhancement associated with it will decrease with its distance from the metal surface. Again, this distance is determined by chemisorption geometry of the molecule on Ag. The absence of expected peaks is also evidenced in Figure 1e and 1f. Spectra miss both 1010 and 1056 cm^{-1} peaks. One or both of the peaks are expected, identifying the cis or trans state or a transition in between, respectively.

Since pR converts into pB on the millisecond time scale, carbonyl flip and protonation markers are expected in the same spectrum. In contrast, as in Figure 1e, the two markers are often not observed together. In addition to the selection rules, a plausible explanation is that isomerization cannot always trigger protonation due to the chromophore's interaction with the nanoparticle surface. For example, if the phenolic oxygen binds with Ag, it may not protonate as quickly or at all.

In conclusion, we have captured the dynamic conformational steps of single PYP molecules using an SERS substrate approach.

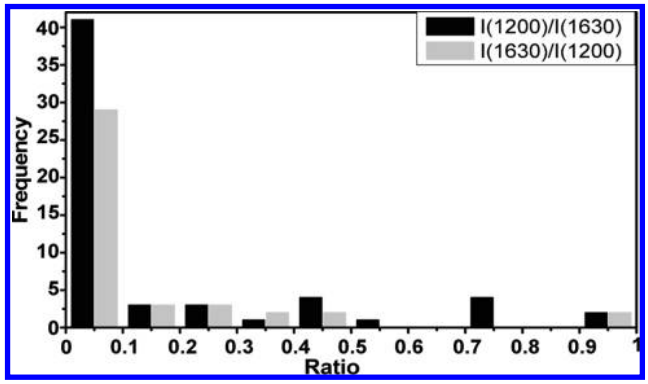

Figure 4. Histogram based upon 100 SM-SERS spectra, each of which captured either the ~1200 or 1630 cm^{-1} peak or both. The ratio is the lower peak intensity divided by larger peak intensity. The bin size is 0.1.

These steps conform to those in PYP's photocycle, already established in the literature. At the SM level, SERS yields well-resolved peaks, some of which were not reported earlier. Further, exclusive peak pairs have been identified that can elucidate PYP's conformational steps and chemisorption configuration on Ag using the SERS selection rules. Despite the "weak chemisorption" of PYP on silver that only allows the SM signal to sustain for ~1 s (followed by its desorption), this duration may be long enough to study PYP's photocycle (~0.3 s).

Acknowledgment. The authors greatly appreciate funding of this work by Oklahoma State Regents for Higher Education and National Science Foundation (Award No. 0756791). They also thank Dr. Aihua Xie and Dr. Wouter Hoff for providing the PYP.

Note Added after ASAP Publication. Additional experimental details were added to the Supporting Information December 2, 2009.

Supporting Information Available: SERS substrate preparation and SERS enhancement factor calculation. This material is available free of charge via the Internet at http://pubs.acs.org.

References

(1) Moerner, W. E. *J. Phys. Chem. B* **2002**, *106*, 910–927.
(2) Nie, S. M.; Emory, S. R. *Science* **1997**, *275*, 1102–1106.
(3) Kneipp, K.; Wang, Y.; Kneipp, H.; Perelman, L. T.; Itzkan, I.; Dasari, R.; Feld, M. S. *Phys. Rev. Lett.* **1997**, *78*, 1667–1670.
(4) Habuchi, S.; Cotlet, M.; Gronheid, R.; Dirix, G.; Michiels, J.; Vanderleyden, J.; Schryver, F. C. D.; Hofkens, J. *J. Am. Chem. Soc.* **2003**, *125*, 8446–8447.
(5) Xu, H. X.; Bjerneld, E. J.; Käll, M.; Borjesson, L. *Phys. Rev. Lett.* **1999**, *83*, 4357–4360.
(6) Bjerneld, E. J.; Földes-Papp, Z.; Käll, M.; Rigler, R. *J. Phys. Chem. B* **2002**, *106*, 1213–1218.
(7) Meyer, T. E. *Biochim. Biophys. Acta* **1985**, *806*, 175–183.
(8) Sprenger, W. W.; Hoff, W. D.; Armitage, J. P.; Hellingwerf, K. J. *J. Bacteriol.* **1993**, *175*, 3096–3104.
(9) Baca, M.; Borgstahl, G. E. O.; Boissinot, M.; Burke, P. M.; Williams, D. R.; Slater, K. A.; Getzoff, E. D. *Biochemistry* **1994**, *33*, 14369–14377.
(10) Borgstahl, G. E. O.; Williams, D. R.; Getzoff, E. D. *Biochemistry* **1995**, *34*, 6278–6287.
(11) Meyer, T. E.; Yakali, E.; Cusanovich, M. A.; Tollin, G. *Biochemistry* **1987**, *26*, 418–423.
(12) Kalkan, A. K.; Fonash, S. J. *J. Phys. Chem. B* **2005**, *109*, 20779–20785.
(13) Singhal, K.; Bhatt, K.; Kang, Z.; Hoff, W.; Xie, A.; Kalkan, A. K. In *Functional Plasmonics and Nanophotonics*; Maier, S., Kawata, S., Eds.; Materials Research Society Symposium Proceedings: Warrendale, PA, 2008; Vol. 1077E, pp 1077-L10-04.
(14) Kalkan, A. K.; Fonash, S. J. *J. Appl. Phys. Lett.* **2006**, *89*, 233103/1.
(15) Bjerneld, E. J.; Johansson, P.; Käll, M. *Single Molecules* **2000**, *1*, 239–248.
(16) Unno, M.; Kumauchi, M.; Tokunaga, F.; Yamauchi, S. *J. Phys. Chem. B* **2007**, *111*, 2719–2726.
(17) Unno, M.; Kumauchi, M.; Sasaki, J.; Tokunaga, F.; Yamauchi, S. *J. Phys. Chem. B* **2003**, *107*, 2837–2845.
(18) Adesokan, A. A.; Pan, D. H.; Fredj, E.; Mathies, R. A.; Gerber, R. B. *J. Am. Chem. Soc.* **2007**, *129*, 4584–4594.
(19) Genick, U. K.; Soltis, S. M.; Kuhn, P.; Canestrelli, I. L.; Getzoff, E. D. *Nature* **1998**, *392*, 206–209.
(20) Xie, A. H.; Hoff, W. D.; Kroon, A. R.; Hellingwerf, K. J. *Biochemistry* **1996**, *35*, 14671–14678.
(21) Xie, A. H.; Kelemen, L.; Hendriks, J.; White, B. J.; Hellingwerf, K. J.; Hoff, W. D. *Biochemistry* **2001**, *40*, 1510–1517.
(22) Lee, B. C.; Pandit, A.; Croonquist, P. A.; Hoff, W. D. *Proc. Natl. Acad. Sci. U.S.A.* **2001**, *98*, 9062–9067.
(23) Hellingwerf, K. J.; Hendriks, J.; Gensch, T. *J. Phys. Chem. A* **2003**, *107*, 1082–1094.
(24) Hoff, W. D.; Vanstokkum, I. H. M.; Vanramesdonk, H. J.; Vanbrederode, M. E.; Brouwer, A. M.; Fitch, J. C.; Meyer, T. E.; Vangrondelle, R.; Hellingwerf, K. J. *Biophys. J.* **1994**, *67*, 1691–1705.
(25) Fromm, D. P.; Sundaramurthy, A.; Kinkhabwala, A.; Schuck, P. J.; Kino, G. S.; Moerner, W. E. *J. Chem. Phys.* **2006**, *124*, 061101.
(26) Smith, E.; Dent, G. *Modern Raman Spectroscopy: A Practical Approach*; John Wiley and Sons, Ltd: West Sussex, U.K., 2005; pp 210−211.
(27) Lombardi, J. R.; Birke, R. L. *J. Phys. Chem. C* **2008**, *112*, 5605–5617.
(28) Xu, H. X.; Aizpurua, J.; Käll, M.; Apell, P. *Phys. Rev. E* **2000**, *62*, 4318–4324.
(29) Persson, B. N. J. *Surf. Sci.* **1993**, *281*, 153–162.
(30) Jackel, F.; Kinkhabwala, A. A.; Moerner, W. E. *Chem. Phys. Lett.* **2007**, *446*, 339–342.

JA9028704